

Review

# Harvesting Thermal Energy through Pyroelectric and Thermoelectric Nanomaterials for Catalytic Applications

Shun Li <sup>1,\*</sup>, Xinbo Liu <sup>1</sup>, Xinyue Zhang <sup>2</sup>, Youling Wang <sup>2</sup>, Shanliang Chen <sup>2,3</sup>, Yong Liu <sup>2,\*</sup> and Yuqiao Zhang <sup>1,\*</sup>

<sup>1</sup> Institute of Quantum and Sustainable Technology (IQST), School of Chemistry and Chemical Engineering, Jiangsu University, Zhenjiang 212013, China; liuxinbo@stmail.ujs.edu.cn

<sup>2</sup> Foshan (Southern China) Institute for New Materials, Foshan 528200, China; zhangxy6191@163.com (X.Z.); youlingwang001@gmail.com (Y.W.); chenshanliang@fscinm.com (S.C.)

<sup>3</sup> Guangdong ENA Technology Inc., Foshan 528200, China

\* Correspondence: shun@ujs.edu.cn (S.L.); liuyong@fscinm.com (Y.L.); yuqiaozhang@ujs.edu.cn (Y.Z.)

**Abstract:** The current scenario sees over 60% of primary energy being dissipated as waste heat directly into the environment, contributing significantly to energy loss and global warming. Therefore, low-grade waste heat harvesting has been long considered a critical issue. Pyroelectric (PE) materials utilize temperature oscillation to generate electricity, while thermoelectric (TE) materials convert temperature differences into electrical energy. Nanostructured PE and TE materials have recently gained prominence as promising catalysts for converting thermal energy directly into chemical energy in a green manner. This short review provides a summary and comparison of catalytic processes initiated by PE and TE effects driven by waste thermal energy. The discussion covers fundamental principles and reaction mechanisms, followed by the introduction of representative examples of PE and TE nanomaterials in various catalytic fields, including water splitting, organic synthesis, air purification, and biomedical applications. Finally, the review addresses challenges and outlines future prospects in this emerging field.

**Keywords:** waste heat; pyroelectric; thermoelectric; nanomaterials; catalysis



**Citation:** Li, S.; Liu, X.; Zhang, X.; Wang, Y.; Chen, S.; Liu, Y.; Zhang, Y. Harvesting Thermal Energy through Pyroelectric and Thermoelectric Nanomaterials for Catalytic Applications. *Catalysts* **2024**, *14*, 159. <https://doi.org/10.3390/catal14030159>

Academic Editor: Carlo Santoro

Received: 15 December 2023

Revised: 31 January 2024

Accepted: 16 February 2024

Published: 21 February 2024



**Copyright:** © 2024 by the authors. Licensee MDPI, Basel, Switzerland. This article is an open access article distributed under the terms and conditions of the Creative Commons Attribution (CC BY) license (<https://creativecommons.org/licenses/by/4.0/>).

## 1. Introduction

### 1.1. Waste Heat Energy

With the rapid development of modern society, the severe environmental contamination and greenhouse effect induced by the consumption of fossil fuel is requiring the revolution of the energy structure in order to realize the Sustainable Development Goals (SDGs) [1,2]. The final destination of all types of energies is heat, which is plentiful and widely accessible from the ambient environment. In nature, heat sources are usually the sunlight, geothermal energy, and exhausted heat from organisms. Moreover, large amounts of extra waste heat are continuously generated from human activities. In the human production process, only 1/3 of the primary energy can be harvested and utilized, leaving 2/3 exhausted as waste heat. Therefore, there is a compelling need to harvest waste heat from the environment, industrial production, and daily life. Exploring new and efficient technologies for waste heat recycling is of great importance for the next generation energy management.

### 1.2. Pyroelectric and Thermoelectric Materials for Converting Waste Heat to Chemical Energy

Basically, both pyroelectric (PE) and thermoelectric (TE) materials can be used for harvesting thermal energy to produce electricity. The difference is that pyroelectric materials need a temporal temperature change, while thermoelectric materials require a temperature gradient. PE materials, as non-centrosymmetric polar crystals whose internal polarization changes through the slight movement of atoms inside the crystal structure depending on temperature, have been widely studied for thermal fluctuations to electric conversion

applications such as infrared temperature detectors [3,4]. On the other hand, in the case of TE materials, when there is a temperature difference at the two ends, the charge carriers tend to move from the high temperature side to the low temperature side, which can realize electricity production [5–8].

In addition to direct electricity generation, recent advances have demonstrated intriguing effects for initiating and promoting catalytic redox reactions by nanostructured PE [9–19] and TE materials, driven by heat fluctuation and temperature difference, respectively. These two effects can be utilized for diverse applications such as pollutant degradation, hydrogen generation, organic synthesis, disinfections, etc. [20–26], through harvesting the universally existing thermal energy in the environment, human body, and industrial production. Thus far, several reviews have been published on the PE catalysis effect [9,27–30], while TE catalysis processes have received less attention. Therefore, a comprehensive review is required to develop a systematical knowledge of these two effects and their ability to utilize waste heat for driving green catalysis processes.

### 1.3. Purpose of This Review

In this review, we develop a comprehensive summary on PE- and TE-driven or -assisted green catalysis driven by waste heat. We mainly focus on the fundamental comparison of these two new catalytic effects, in terms of materials candidate, working condition, mechanism, and potential application, by presenting the most representative examples reported up until now. Firstly, we start with the introduction of the fundamentals and basic principles behind the PE and TE effects. Then, the recent progress in the materials and applications of PE and TE catalysis are presented. Finally, potential ways to further promote the catalytic performance along with a brief outlook are proposed. A comparison of these two catalytic effects is listed in Table 1. The potential applications of PE and TE catalysis effects are illustrated in Figure 1, presenting the utilization of waste heat from the natural environment, industry, and daily life to drive different catalytic reactions in the field of clean energy production, environmental remediation, and disinfections.

**Table 1.** Comparison of PE and TE catalysis.

	Materials	Working Condition	Mechanism
PE catalysis	Pyroelectric materials	Temperature fluctuation	Polarization charges
TE catalysis	Thermoelectric materials	Temperature gradient	Thermal-excited free charges

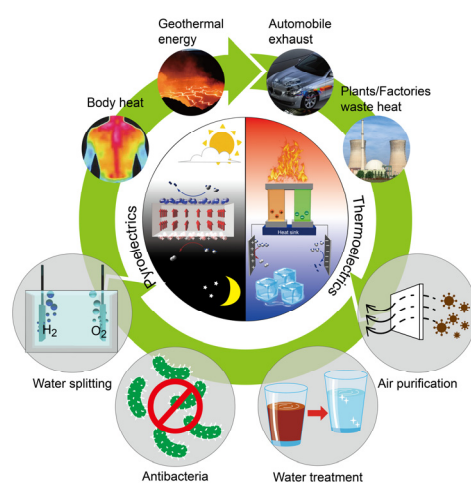


**Figure 1.** Pyroelectric and thermoelectric catalysis for various applications.

## 2. Pyroelectric Catalysis

### 2.1. Pyroelectric Effect

Among the 32 crystalline point groups, 21 show non-centrosymmetry with piezoelectricity, and 10 out of the 21 point groups correspond to PE materials [31]. Without an external electric field, there is spontaneous polarization ( $P_s$ ) existing in PE materials, which will change depending on temperature ( $T$ ). Therefore, under a temperature fluctuation, the charges accumulated on the surface of PE materials will change with their internal polarization.

Figure 2a summarizes an illustration of PE effect in response to the temperature oscillation. At the temperature below Curie temperature ( $T_c$ ), the system can hold its spontaneous polarization. As the temperature increases ( $dT/dt > 0$ ), the  $P_s$  experiences a declining tendency due to the loss of electric dipoles, resulting in an imbalance between screening charges and polarization charges. To compensate the imbalance, a current flow will be generated under a short-circuit condition, or a potential difference will exist under an open-circuit condition. On the contrary, in a cooling condition ( $dT/dt < 0$ ),  $P_s$  increases with decreasing temperature. The screening charges redistribute to the surface, resulting in a current or electric field in the reverse direction. At a constant temperature ( $dT/dt = 0$ ), the built-in electric field is always balanced by screening charges at the surface. In this case, there is no electric potential or current [9,28].

### 2.2. Mechanism and Key Factors of Pyroelectric Catalysis

Temperature variation is the driving force for the PE catalysis process. As illustrated in Figure 2b, the PE polarization can be modulated by changing the temperature, generating the positive and negative charges that can induce surface electrochemical catalytic reactions [32]. The temperature oscillation breaks the thermodynamic equilibrium in PE materials, which will be reestablished due to the change of polarization states. Consequently, adsorption/desorption of species from the electrolyte alternatively occur on the surface of PE materials, resulting in more free carriers that participate in the redox reactions, and the PE catalytic reaction continues. Therefore, the PE catalysis process provides a green route to utilize waste heat from nature, such as day and night temperature alternation.

For PE materials, the PE coefficient ( $p$ ) that indicates the charge release can be expressed as

$$p = dP_s/dT \quad (1)$$

As the temperature approaches  $T_c$ ,  $p$  tends to be maximized. And when the temperature is above  $T_c$ ,  $p$  returns to zero, since the ferroelectric state has been broken. Based on  $p$ , the PE current ( $I$ ) and potential ( $dV$ ) across a PE material with a thickness of  $d$  and a surface area of  $A$  under an open-circuit condition can be expressed as

$$I = p \times A \times dT/dt \quad (2)$$

$$dV = p \times d \times dT/\epsilon_{33} \quad (3)$$

where  $\epsilon_{33}$  is the material permittivity at constant stress.

The thickness of PE materials is crucial for the catalytic process. Through modulating the dimension or microstructure of the materials, it is possible to tune the PE catalytic performance. The direct relationship between the electric field strength and voltage is readily apparent. Consequently, in the PE catalysis process, oxidation and reduction reactions occur when the electric field strength reaches a sufficient level to ensure that the corresponding voltage meets the requisite potential threshold. This principle is pivotal and must be carefully considered in the design of PE catalysts. Second, temperature change as the energy source is needed during the PE catalysis process. For the traditional PE materials used as energy harvesters or sensors, researchers seek materials with high  $T_c$  that will hold their polarization even at harsh conditions (i.e.,  $T > 100$  °C). However, in the case of the PE catalysis processes, low- $T_c$  materials are favored since the PE effect is

always maximized near  $T_c$ . With the development of materials by rational design and modification, pyroelectricity and suitable  $T_c$  can be optimized, which improves the PE catalytic performance.

Experimentally, there are two ways to couple PE effect with electrochemical reactions. The first: PE modules perform as “batteries” outside the reaction environment, which firstly convert temperature oscillation into electricity and then support the electrochemical redox through an external circuit [14–16,33]. Using a rectification circuit, a constant current could be kept holding the same type of reaction at a single electrode regardless of the periodically changed current direction depending on the temperature oscillation. The second way is by exploiting nanostructured PE materials to participate in the electrochemical reactions by directly contacting the reactants and periodically realizing the catalysis at the same surface depending on the temperature fluctuations.

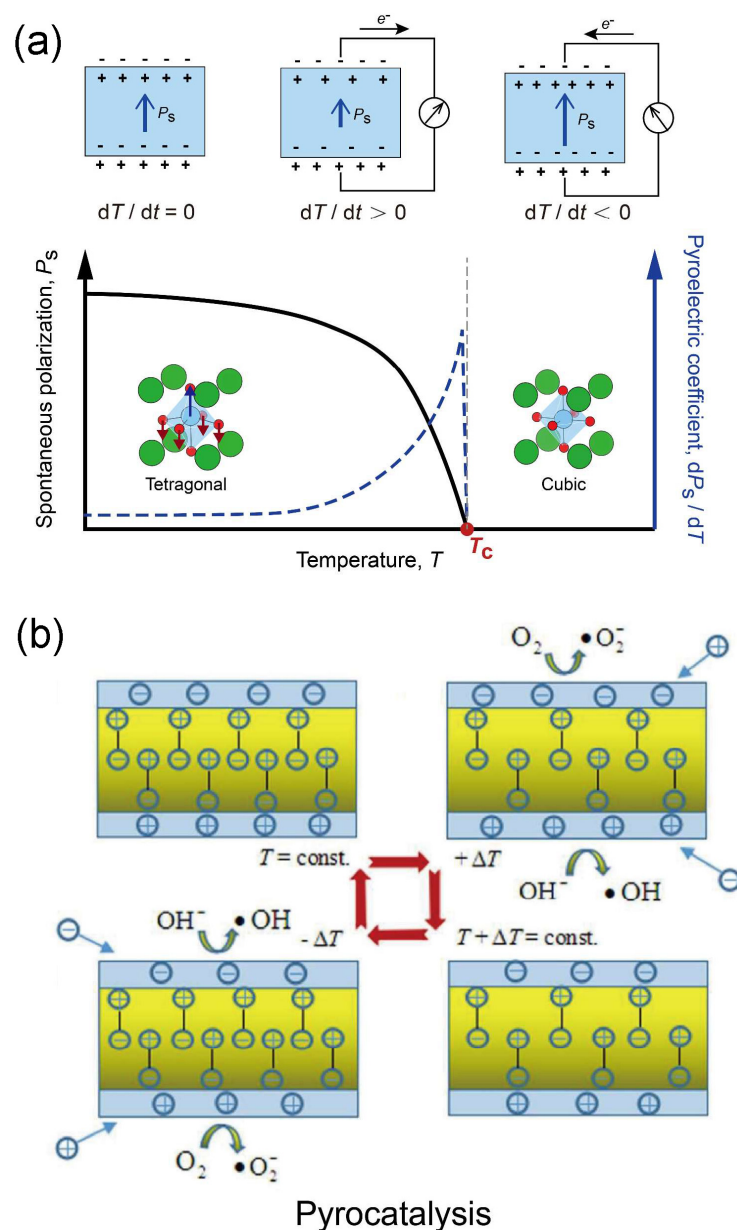


**Figure 2.** Schematic illustration of (a) PE effect and (b) PE catalysis mechanism. Reproduced from [28,34]. Copyright © Cell press, 2020; Royal Society of Chemistry, 2016.

### 2.3. Recent Progress in Pyroelectric Catalysis

Based on the principle above, a great number of works both theoretical and experimental have been published so far [11–16,32,33,35–40]. In this section, recent key progress of PE nanomaterials for diverse catalysis areas, including water splitting, CO<sub>2</sub> reduction, biomedical applications, etc., will be discussed.

In 2016, Kakekhani et al. conducted a density function theory (DFT) calculation on the PE catalysis of PbTiO<sub>3</sub> towards the decomposition of NO<sub>x</sub> and oxidation of SO<sub>2</sub>, proposing electrochemical redox under cyclically changing polarization conditions [35–37]. These are the pioneering works in modelling the PE effect in electrochemical reactions.

The PE catalysis process has been utilized for water splitting to produce hydrogen, as exemplified by Ba<sub>0.7</sub>Sr<sub>0.3</sub>TiO<sub>3</sub> (BST) nanoparticles and CdS nanorods [32,40]. Xu et al. [32] demonstrated the pyrocatalytic H<sub>2</sub> production using BST NPs. The H<sub>2</sub> yield was about 46.89 μmol·g<sup>-1</sup> after 33 thermal cycles in the temperature range of 25 to 50 °C. In addition, PE catalytic water splitting was also reported in other materials, such as BaTiO<sub>3</sub> [41] and 2D black phosphorene [19]. Very recently, Au/BaTiO<sub>3</sub> composite achieved a high H<sub>2</sub> production rate of about 133 μmol·g<sup>-1</sup>·h<sup>-1</sup> under pulsed laser irradiation [41] (Figure 3). Both experimental and theoretical analysis revealed that plasmonic local heating is a highly efficient way to drive PE catalysis reactions.

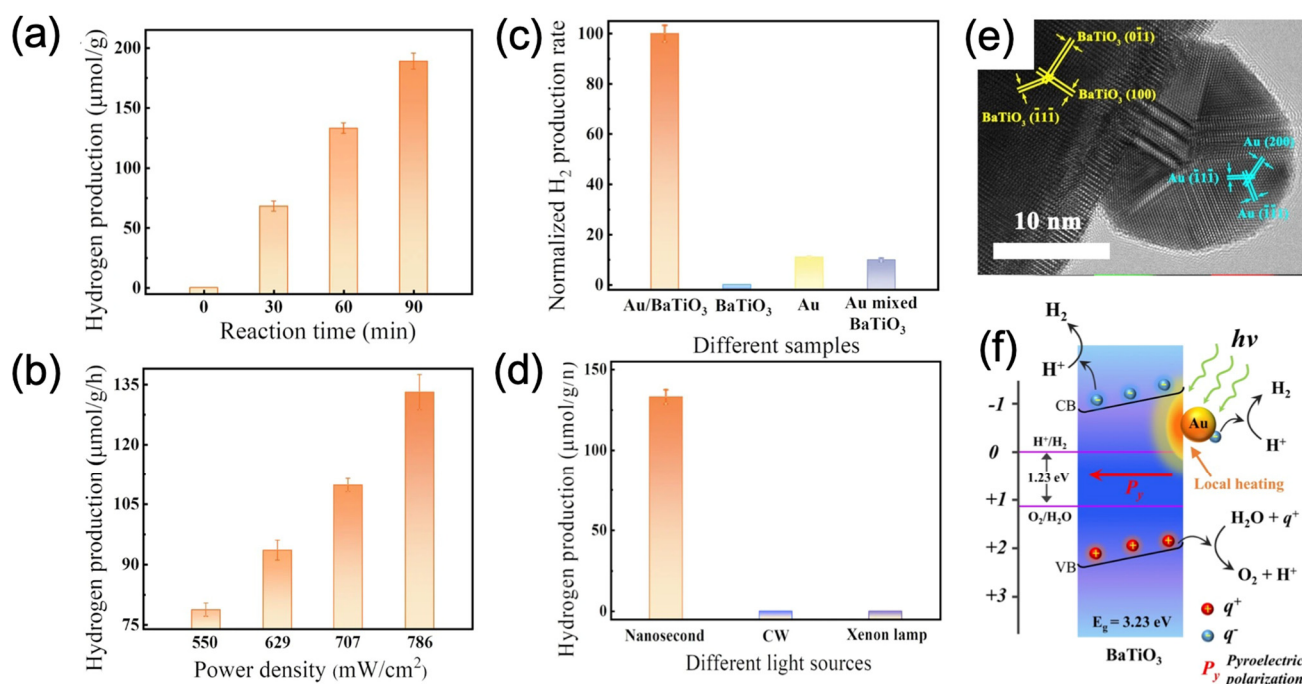


**Figure 3.** (a–d) PE catalytic water splitting for H<sub>2</sub> generation by Au/BaTiO<sub>3</sub> nanocomposites under different conditions. (e) HR-TEM image of the Au/BaTiO<sub>3</sub> nanocomposites. (f) Schematic illustration of the mechanism for PE catalytic H<sub>2</sub> generation using Au/BaTiO<sub>3</sub> nanocomposites driven by surface plasmon local heating. Reproduced from [41]. Copyright © Nature Publishing Group, 2022.

In addition to H<sub>2</sub> production, PE nanostructured materials have also been utilized to reduce CO<sub>2</sub> to methanol. For example, it was reported that layered perovskite Bi<sub>2</sub>WO<sub>6</sub> nanoplates can harvest heat energy from temperature variation, driving PE catalytic CO<sub>2</sub> reduction for methanol at temperatures between 15 °C and 70 °C [42] (Figure 4). The methanol yield was 55.0 μmol·g<sup>-1</sup> after 20 temperature-changing cycles. This low-cost and green catalytic CO<sub>2</sub> reduction strategy provides a new route towards clean energy production utilizing natural temperature variation.

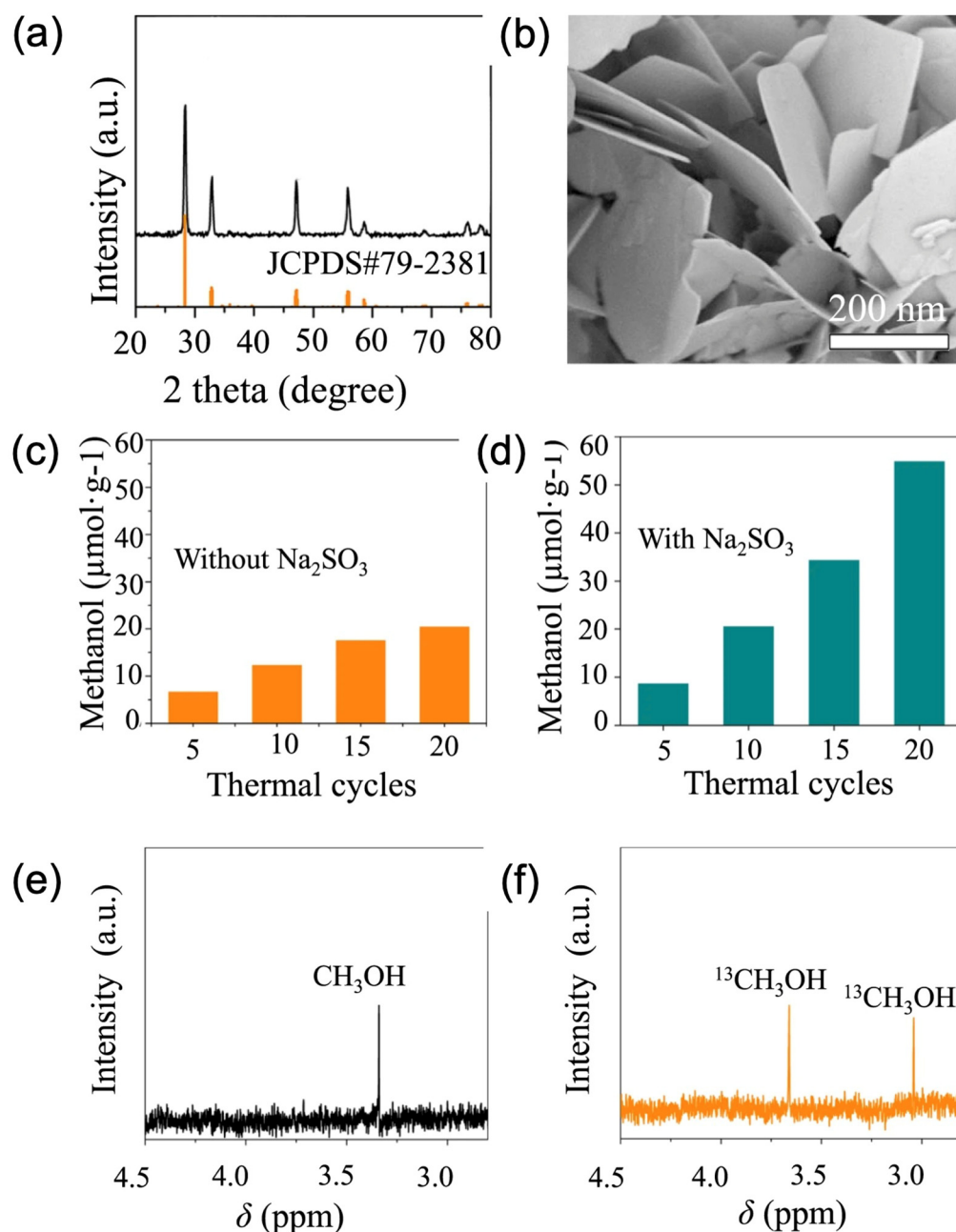


**Figure 4.** (a) XRD pattern and (b) SEM image of Bi<sub>2</sub>WO<sub>6</sub> nanosheets. PE catalytic CO<sub>2</sub> reduction for producing methanol (c) without Na<sub>2</sub>SO<sub>3</sub> and (d) with Na<sub>2</sub>SO<sub>3</sub> as sacrificial agent. The <sup>1</sup>H NMR spectra with (e) unlabeled CO<sub>2</sub> and (f) labeled <sup>13</sup>CO<sub>2</sub>. Copyright © Nature Publishing Group, 2022. Reproduced from [42]. Copyright © Nature Publishing Group, 2021.

Beyond clean energy production, PE catalysis strategy has been also proven effective for biomedical applications such as tooth whitening [18]. In 2022, Wang et al. demonstrated a non-destructive and biocompatible tooth whitening strategy based on BaTiO<sub>3</sub> nanowire-based PE composite hydrogel (Figure 5). It was found that teeth stained with different agents were completely whitened with BaTiO<sub>3</sub> nanowire turbid liquid after 2000 thermal cycles with a temperature fluctuation of 25 °C. Moreover, a prototype tooth whitening dental brace using BaTiO<sub>3</sub> nanowires combined with light-cured hydrogel showed excellent chemical and structural stability. This work highlights the great prospects of a simple and low-cost tooth whitening route by utilizing PE nanomaterials without additional equipment.

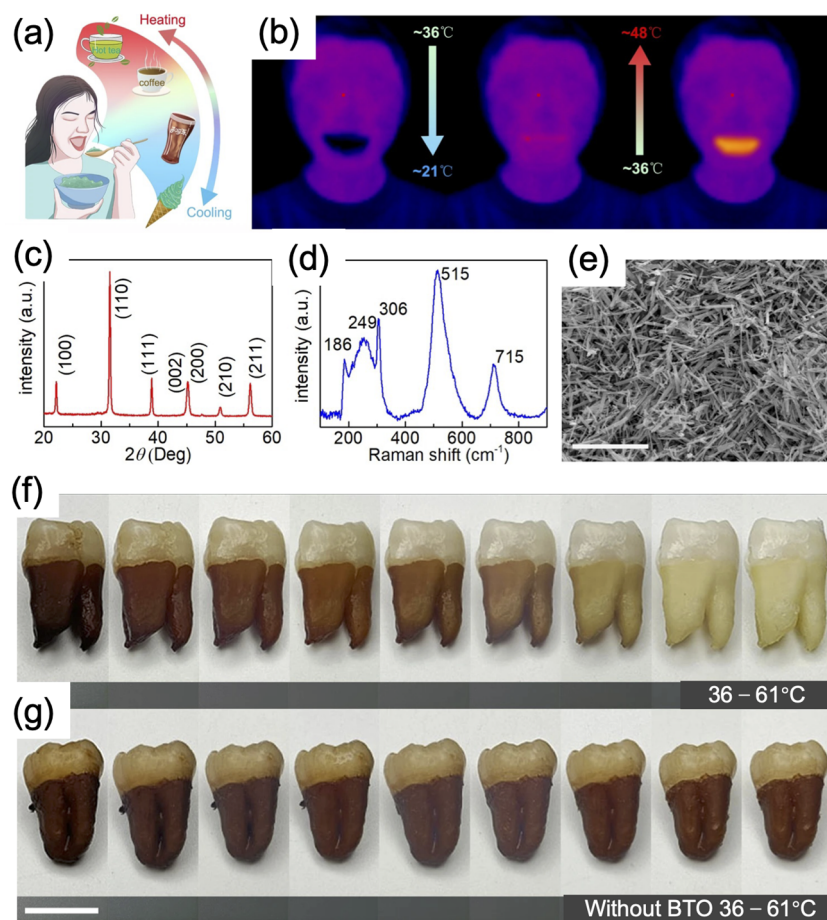


**Figure 5.** (a) Illustration of temperature changes in oral environment. (b) Infrared imaging of the temperature change in oral environment after drinking cold and hot water. (c) XRD pattern, (d) Raman spectra and (e) SEM images of BaTiO<sub>3</sub> nanowires. (f) Photographs of teeth under treatment in turbid liquid of BaTiO<sub>3</sub> nanowires with a temperature fluctuation of 25 °C. (g) Photographs of teeth under treatment in pure water with a temperature fluctuation of 25 °C. Reproduced from [18]. Copyright © Nature Publishing Group, 2022.

Furthermore, the PE catalytic effect can also be applied to the synthesis of heterostructures. Through the PE effect, Liu et al. synthesized Ag/Pt/Pd/Au-BaTiO<sub>3</sub> hybrid nanoparticles by dispersing BaTiO<sub>3</sub> nanoparticles in an AgNO<sub>3</sub>/K<sub>2</sub>PtCl<sub>4</sub>/Na<sub>2</sub>PdCl<sub>4</sub>/HAuCl<sub>4</sub> solution under fast temperature vibrations. The metal-BaTiO<sub>3</sub> hybrid nanoparticles in turn displayed better PE catalytic degradation efficiency of the dye solution [11]. This method provides a new way of synthesizing metal-PE materials without the need for additional reducing reagents.

### 3. Thermoelectric Catalysis Effect

#### 3.1. Thermoelectric Effect

The development and application of TE materials has been a hotspot in the past few decades due to the increasing global energy demand [43–46]. Based on the Seebeck effect, TE materials can perform as energy suppliers by converting the temperature gradient into electricity. As shown in Figure 6a, when a temperature difference ( $\Delta T$ ) is introduced to both ends of a TE material, the charge carriers will be driven to move from the hot side to the cold side. Correspondingly, a potential difference ( $\Delta V$ ) is generated.  $\Delta V$  is proportional to  $\Delta T$ , and their ratio is called the Seebeck coefficient ( $S = \Delta V / \Delta T$ ). The overall performance of TE materials can be evaluated by a dimensionless figure of merit,  $ZT$ , expressed as

$$ZT = S^2 \times \sigma \times T / \kappa \quad (4)$$

where  $\sigma$  is electrical conductivity,  $\kappa$  is thermal conductivity, and  $T$  is the absolute temperature. The  $ZT$  of representative TE materials such as  $\text{Bi}_2\text{Te}_3$  and  $\text{PbTe}$  is  $\approx 1$ , which is currently believed to be the standard requirement for practical applications [47,48]. In pursuit of high conversion efficiency, several materials with high  $ZT$  values have been proposed recently, most of which are semiconductors with ultralow  $\kappa$ , including  $\text{Bi}_2\text{Te}_3$  [49–51],  $\text{PbTe}$  [52,53],  $\text{SnSe}$  [7,54,55],  $\text{BiCuSeO}$  [56,57],  $\text{AgSbSe}_2$  [58], etc.

### 3.2. Thermoelectric Catalytic Effect

In addition to TE electricity generators, direct coupling of the TE effect and electrochemical process is a promising research direction for TE materials, since semiconductor-based electrochemical reactions mostly take place under mild conditions [59]. The voltage generated at a small temperature gradient in TE materials with large  $S$  can match most of the reaction threshold in electrochemical redox. Unlike the PE materials that require a constantly changing temperature with time, TE materials can keep a constant output if there is a stable temperature gradient. The first report of TE effect-assisted water splitting dates back to 1976, when solar energy was adopted as the heating source [60]. In this work, the TE electricity generator is independent from the electrochemical reactor, performing as a TE electricity generator assisting a photochemical cell for an electrolytic tank. In this system, the efficiency of the TE generator is only 5%, but the total hydrogen production could be increased by 20% [61]. Pornrunroj et al. demonstrated that photoelectrochemical reactors can utilize this waste heat by integrating thermoelectric modules, which provide additional voltage under concentrated light irradiation [62]. This thermal management approach enables unassisted overall water splitting, even for PEC systems with insufficient photovoltage. As the external type of TE effect applied in electrochemical redox, it still cannot get rid of the large amount of energy lost and the low efficiency during conversion between heat and electricity. Therefore, in recent years, researchers are changing the focus on TE materials to driving intrinsic catalysis induced by temperature difference (Figure 6b), making nanostructured TE materials to directly participate in the electrochemical redox reactions.

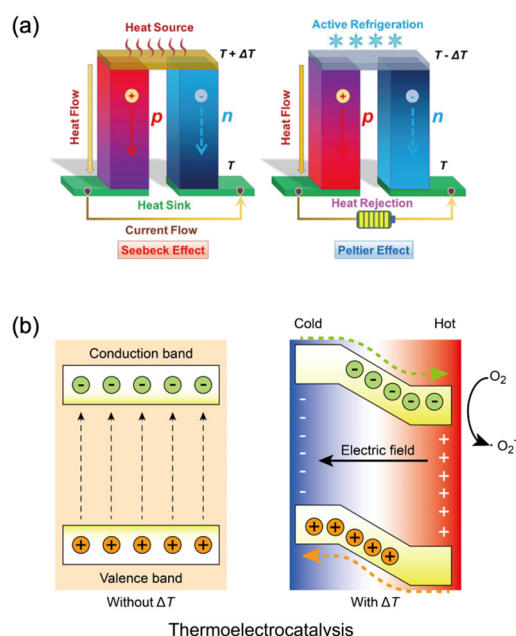


**Figure 6.** Schematic illustration of (a) TE effect and (b) TE catalysis mechanism. Reproduced from [22,63]. Copyright © Nature Publishing Group, 2021; American Chemical Society, 2020.

### 3.3. Recent Progress in Thermoelectric Catalysis

In 2017, Sharifi et al., for the first time, experimentally demonstrated a novel thermoelectrocatalysis effect [24]. In their work,  $\text{Sb}_2\text{Te}_3$  and  $\text{Bi}_x\text{Sb}_{2-x}\text{Te}_3$  nanosheets were

synthesized and assembled into a three-electrode electrochemical cell (Figure 7). By applying a temperature gradient of  $\sim 90^\circ\text{C}$ , a remarkable improvement in the increasing rate of current density by voltage was observed, and the current density ( $-0.6\text{ V vs. RHE}$ ) was 7 times higher than its value without a temperature gradient. Therefore, the electrocatalytic current can be promoted using nanostructured TE materials in a hydrogen evolution reaction (HER) by the thermoelectricity generated from temperature gradients. This finding opens an entirely new way of utilizing TE materials to participate in electrochemical redox reactions by directly contacting the reagents or electrolytes rather than performing as external batteries. Inspired by this pioneering work, a number of studies have been carried out on nanostructured TE materials as electrochemical catalysts [64,65]. In the following parts, we will present some representative examples that utilize this new catalytic effect for driving various redox reactions.

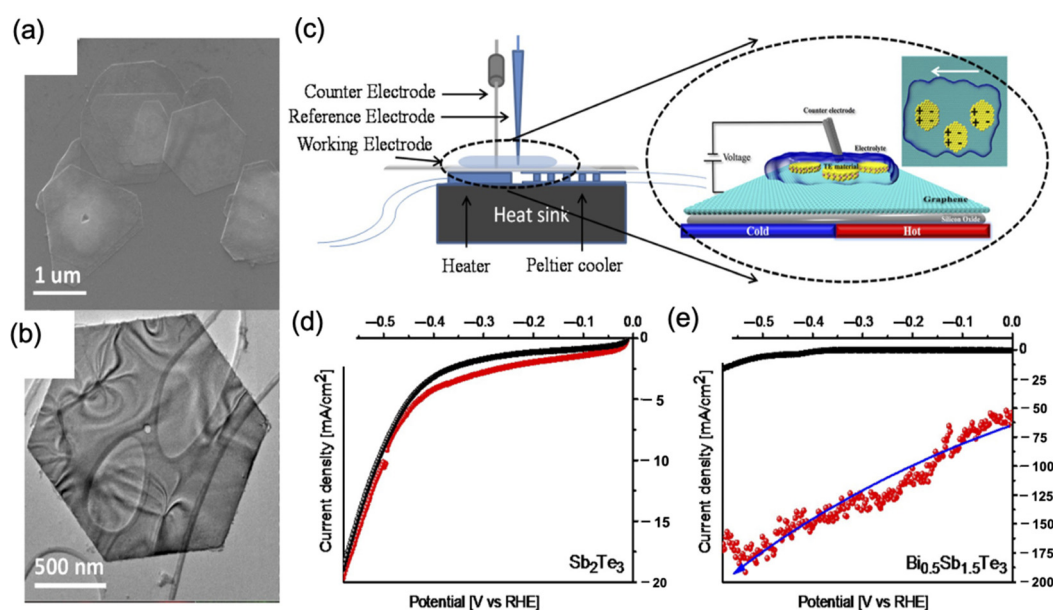


**Figure 7.** (a) SEM and (b) TEM images of  $\text{Bi}_{0.5}\text{Sb}_{1.5}\text{Te}_3$  nanosheets. (c) Schematic illustration of electrochemical cell placed on top of a TE generator system with a Peltier cooler and a thin heater. Electrochemical measurements under different temperature gradients of (d)  $\text{Sb}_2\text{Te}_3$  and (e)  $\text{Bi}_{0.5}\text{Sb}_{1.5}\text{Te}_3$ . Reproduced from [24]. Copyright © American Chemical Society, 2017.

For example, Achour et al. proposed a new concept of TE promotion of catalysis (TEPOC), which is based on non-Faradaic electrochemical modification of catalytic activity (NEMCA) [20]. The NEMCA, which involves a reversible change of catalytic properties of metal catalysts deposited on solid electrolytes, can be obtained by applying a small external electric current or voltage. Based on this principle, they proposed to use a TE material to change the effective work function of catalyst particles to achieve a significant increase in the catalytic activity of  $\text{CO}_2$  hydrogenation. They developed an innovative use of a mid-temperature TE material,  $\text{BiCuSeO}$  (a well-known oxide-based TE material showing high  $S$  along with low  $\kappa$  [56,57]), as a supporter and promoter of a Pt catalyst for  $\text{CO}_2$  hydrogenation. As shown in Figure 8, they set up a reactor by placing the reaction chamber on top of a hot plate to create a large temperature difference ( $\sim 200$  to  $300\text{ K}$ ) between the bottom floor of the chamber and the hot surface of the  $\text{BiCuSeO}$  plate. As a result, the author obtained a much higher catalytic efficiency at a larger temperature gradient, suggesting a NEMCA from  $\text{BiCuSeO}$ . From a linear relationship between the logarithm of the reaction rate and the TE Seebeck voltage, it was proposed that the TE effect can change the Fermi level and therefore the work function of the electrons in the catalyst particles supported on a TE material, leading to an exponential increase in catalytic activity.

The authors also applied the same strategy for ethylene oxidation and found a significantly promoted reaction rate by tuning the TE Seebeck voltage [31].

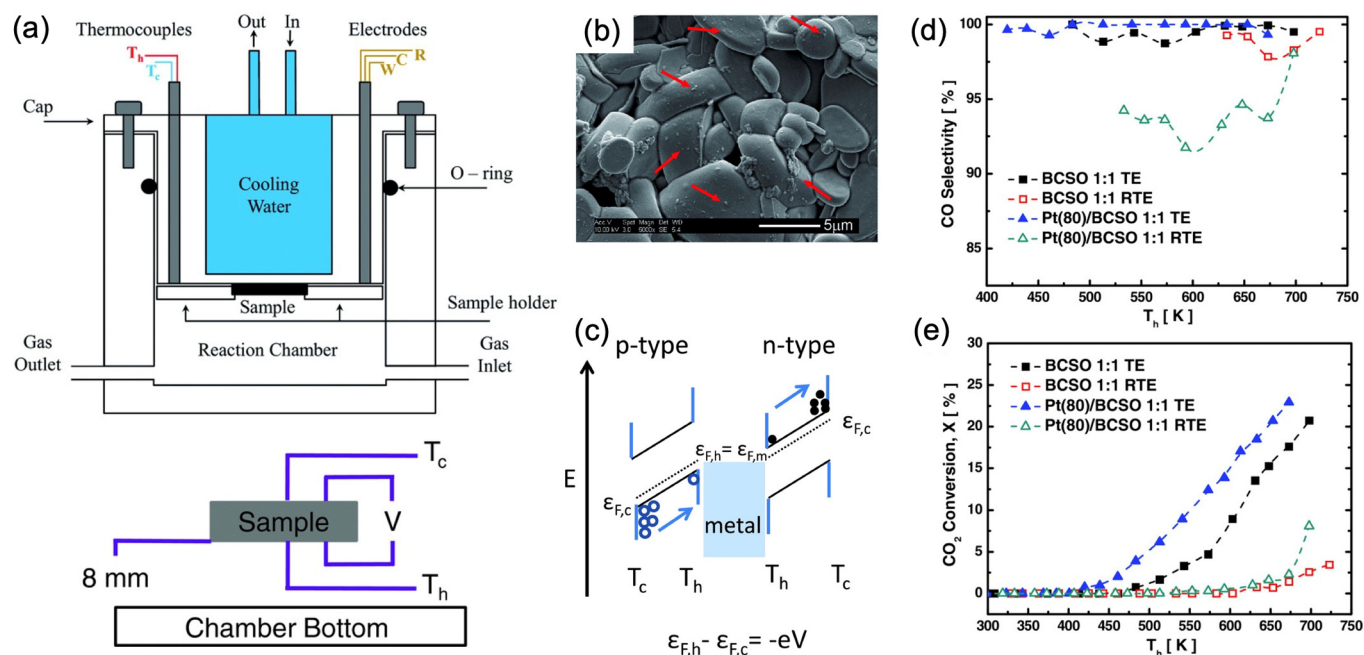


**Figure 8.** (a) Schematic diagram of the single chamber reactor, which combines TE effect with catalytic reaction. (b) SEM image of Pt/BiCuSeO. (c) Energy levels of electrons in a TE material with a temperature gradient. (d) CO selectivity and (e) CO<sub>2</sub> conversion for Pt/BiCuSeO and BiCuSeO. Reproduced from [20]. Copyright © John Wiley & Sons, 2017.

TE effect-assisted electrochemical redox has also been found effective for biomedical applications such as disinfections and cancer therapy [66]. In 2021, Lin et al. reported an excellent hydrogen peroxide generation and environmental disinfection by utilizing Bi<sub>2</sub>Te<sub>3</sub>, one of the most widely studied TE materials [22]. It was found that Bi<sub>2</sub>Te<sub>3</sub> nanosheets can produce H<sub>2</sub>O<sub>2</sub> under a temperature gradient, since the conduction band potential is more negative than the redox potential of O<sub>2</sub>/·O<sub>2</sub><sup>-</sup>. With a TE effect-induced built-in electric field, the thermally activated negative charges rush from the hot side to the cold side of the material. Therefore, the band energy decreases at the positive potential side and increases at the negative potential side, tilting both the valence band and conduction band across the material. The conduction band comes very close to the redox potential for generating ·O<sub>2</sub><sup>-</sup> radicals. Electrons from the conduction band can easily migrate to the solution and produce H<sub>2</sub>O<sub>2</sub> (Figure 9). They also tested some typical TE materials (Bi<sub>2</sub>Te<sub>3</sub>, Sb<sub>2</sub>Te<sub>3</sub> and PbTe) in comparison to TiO<sub>2</sub> with no TE effect, confirming the crucial role of the TE effect. The best performance was obtained in Bi<sub>2</sub>Te<sub>3</sub>, and the catalytic efficiency increased with the increasing temperature gradient. Furthermore, the authors fabricated Bi<sub>2</sub>Te<sub>3</sub> nanoplates on carbon fiber fabric (CFF) and developed a thermocatalytic filter with antibacterial function, which showed excellent and stable disinfection performance under a temperature gradient for over 30 days.

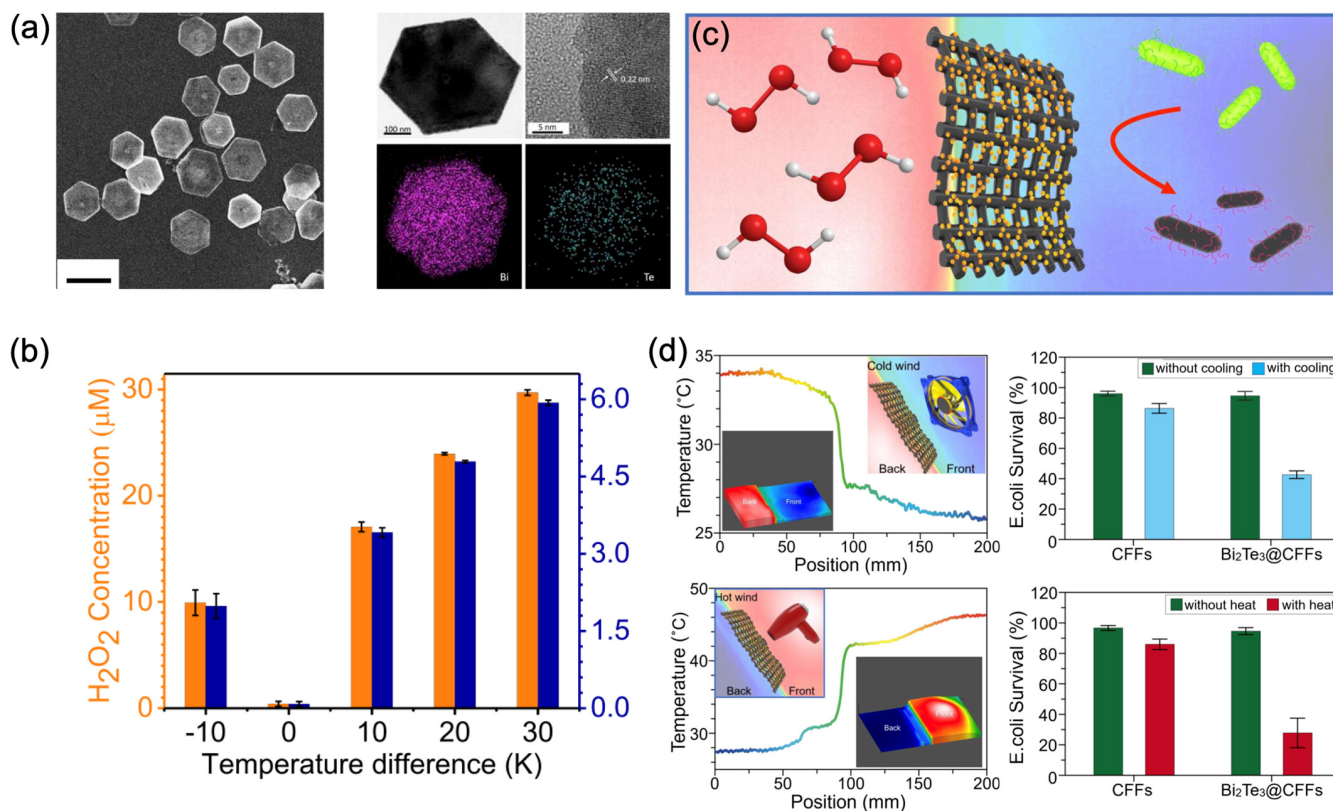


**Figure 9.** (a) SEM and TEM images of Bi<sub>2</sub>Te<sub>3</sub> nanoplates (NPs). (b) H<sub>2</sub>O<sub>2</sub> generation using the Bi<sub>2</sub>Te<sub>3</sub> NPs under various temperature differences. (c) Schematic illustration of the thermocatalytic filter. (d) Temperature profile of the thermocatalytic filter captured by an IR camera during exposure to cold air and hot air and the corresponding disinfection performance. Reproduced from [22]. Copyright © Nature Publishing Group, 2021.

TE effect-assisted disinfection was also reported in SrTiO<sub>3</sub>/Cu<sub>2</sub>Se p-n heterojunction for an efficient TE cancer therapy using laser irradiation as the heating source [67]. Very recently, electrospinning membranes containing rGO-Bi<sub>2</sub>Te<sub>3</sub> nanosheets were shown to exhibit high antibacterial efficiency in vivo ( $99.35 \pm 0.29\%$ ), accelerated tissue repair ability, and excellent biosafety. This study provided an insight into heterointerface design in photo-thermoelectric catalysis [25]. In addition, thermoelectric nanostructured heterojunction of Bi<sub>0.5</sub>Sb<sub>1.5</sub>Te<sub>3</sub>/CaO<sub>2</sub> nanosheets combined with catalytic therapy, ion interference therapy, and immunotherapy demonstrate excellent antitumor performance in female mice [68].

The optimization of air electrodes in zinc–air batteries (ZABs) is crucial for improving their energy efficiency and overcoming challenges such as sluggish kinetics and mutual interference of oxygen evolution and reduction reactions. Zheng et al.’s recent work presents a novel approach to addressing these issues by introducing a new breathing air-electrode configuration in rechargeable ZABs. This configuration utilizes both P-type and N-type TE materials as charge and discharge electrodes, respectively [65]. Due to thermoelectrically generated Seebeck voltages and carrier accumulation, the intrinsic oxygen catalytic activity undergoes a notable enhancement. As a result, the breathing ZABs showcase a remarkable reduction in the charge/discharge voltage gap alongside improved energy efficiency. This work highlights the potential for future advancements in rechargeable zinc–air battery technology.

#### 4. Future Prospects

Coupling PE or TE effect with electrochemical catalysis is a promising approach to convert thermal energy into chemical energy, especially to utilize the “waste heat” in nature. On one hand, PE catalysis effect has the advantages of utilizing temperature

fluctuations, such as the different sunlight irradiation conditions of daytime and night and temperature vibrations from atmospheric circulation/ocean currents. Compared with PE electrochemical catalysis, TE electrochemical catalysis is a relatively new direction in utilizing waste heat with constant temperature difference. The temperature gradient from both nature and industry can provide the driving force for TE electrochemical redox. Even though a number of excellent works have been performed, the study of PE and TE catalysis is still in the primary stage, and the efficiency is still far from the commercial requirement. Further potential ways to improve the PE catalytic performance still need to be explored.

#### (1) PE catalysis.

It is important to develop new PE material systems (e.g., 2D materials) and tailor the PE catalytic performance by modulating the microstructure and exposed crystal facets. By advanced synthesis techniques, it is possible to optimize the PE catalysis activity in different material candidates through quantum confinement, epitaxial strains, etc.

Searching for PE materials with low  $T_c$  is also a promising direction for the development of high-efficiency PE catalysts, since most of the temperature oscillations in nature are mild in form, like temperature changes of the atmosphere between daytime and night, temperature fluctuation in bodies of water, and even organism temperature fluctuations.

The previous studies on PE catalysis lack the quantitative analysis of energy input and calculation of thermo-to-chemical energy conversion efficiency. In the future, multiple effects can be coupled with the PE effect to utilize diverse types of energies. For example, coupling with photocatalysis involves solar energies, and coupling with piezoelectric catalysis can combine mechanical vibrations [69,70].

#### (2) TE catalysis.

The TE catalytic effect is a rather new phenomenon. The role of materials, manufacturing methods, and ZT values on their TE catalytic performance need to be clarified. First, the TE catalytic performance is sensitively dependent on the TE properties of materials. Therefore, searching for materials with both high TE performance and feasible redox potential is important for developing TE catalysts. For example, in the case of water splitting, many wide-band gap semiconductors are possible candidates, like  $\text{TiO}_2$ ,  $\text{SrTiO}_3$ ,  $\text{ZnO}$ , etc. With proper doping, these materials can be turned into TE materials. For example, it has been found that Nb/La-doped  $\text{SrTiO}_3$  shows very high  $S$  due to the heavy effective mass of Ti 3d orbital [71–73]. Adopting these materials can simultaneously fulfill high  $S$  and suitable band structure, bringing enhanced performance. Second, quantum size effect has been proven effective in enhancing the performance of TE materials. Hicks and Dresselhaus proposed a low-dimensional enhancement effect of TE performance by decreasing the dimension of TE materials below the de Broglie wavelength of the charge carriers, which could create a boost in  $S$  without sacrificing  $\sigma$  [71,74–76]. At the same time, attributed to the boundary scattering, low-dimensional materials also display much lower  $\kappa$  than the bulk samples. Combining the quantum confinement effect into TE catalysis may also be an effective way to further improve the TE catalytic performance.

Despite recent progress, understanding of the fundamental mechanisms that govern thermal-to-chemical energy conversion and the design of optimal TE catalytic materials is in the early stages. The accurate evaluation of the overall thermal-to-chemical energy conversion efficiency in nanostructured TE materials has not been realized yet. Another great challenge that limits the application of TE catalysts is the difficulty of forming a steady and controllable temperature gradient at the nano-/microscale.

The previous research efforts on TE catalytic materials indeed hold significant promise for advancing catalytic applications in many fields. Herein, we attempt to delve deeper into some potential application scenarios. For example, one can use the temperature difference between a chamber and the outside ambient environment to drive chemical reactions, placing TE nanomaterials on the inner surface of the reactors. In addition, TE materials may also offer an alternative approach to convert exhaust gases from automobiles into non-toxic byproducts by utilizing TE materials within the exhaust system, driven by the

high temperature difference between inside and outside. This application could lead to the development of more economical exhaust systems for vehicles, potentially replacing conventional noble metal-based catalysts. Moreover, TE nanomaterials are promising for biomedical applications, utilizing the small temperature difference of human body and the surrounding environment.

In summary, with potential applications in a variety of catalysis processes, PE and TE catalytic materials and devices are being studied extensively. Our perspective provides a summary of the state-of-the-art research in this emerging interdisciplinary field, describes the key advances, and illustrates the potential applications of PE and TE catalytic material systems. Its promising prospects in energy, environmental, and biomedical technologies in a wide array of temperature ranges define an opportunity to combine waste heat harvesting and green catalysis processes into industrial production and environmental protection. By leveraging PE and TE catalytic materials, it becomes feasible to initiate and sustain chemical reactions efficiently. This green catalytic technology will greatly promote waste heat energy utilization efficiency. Further research and development in this area holds the potential to revolutionize catalysis and contribute to sustainable technological advancements.

**Author Contributions:** Conceptualization, S.L. and Y.Z.; writing—original draft preparation, Y.Z.; writing—review and editing, S.L., X.L., X.Z., Y.W., S.C. and Y.L.; supervision, Y.L. and Y.Z.; funding acquisition, S.L., Y.L. and Y.Z. All authors have read and agreed to the published version of the manuscript.

**Funding:** The authors would like to acknowledge support from the National Natural Science Foundation of China (Grant No. 22075126, 52202242 and 52172187), the Guangdong Basic and Applied Basic Research Foundation (2020A1515110557), the Guangdong-Macao joint funding program for science and technology innovation (2022A0505020025), and the Start-Up Fund of Jiangsu University (Grant No. 5501310015).

**Data Availability Statement:** No new data were created or analyzed in this study. Data sharing is not applicable to this article.

**Conflicts of Interest:** Dr. Chen S. was employed by the Guangdong ENA Technology Co., Ltd. The remaining authors declare that the research was conducted in the absence of any commercial or financial relationships that could be construed as a potential conflict of interest.

## References

1. Griggs, D.; Stafford-Smith, M.; Gaffney, O.; Rockström, J.; Öhman, M.C.; Shyamsundar, P.; Steffen, W.; Glaser, G.; Kanie, N.; Noble, I. Sustainable development goals for people and planet. *Nature* **2013**, *495*, 305–307. [[CrossRef](#)] [[PubMed](#)]
2. LeBlanc, S. Thermoelectric generators: Linking material properties and systems engineering for waste heat recovery applications. *Sustain. Mater. Technol.* **2014**, *1–2*, 26–35. [[CrossRef](#)]
3. Bowen, C.R.; Taylor, J.; LeBoulbar, E.; Zabek, D.; Chauhan, A.; Vaish, R. Pyroelectric materials and devices for energy harvesting applications. *Energy Environ. Sci.* **2014**, *7*, 3836–3856. [[CrossRef](#)]
4. Zhang, D.; Wu, H.; Bowen, C.R.; Yang, Y. Recent Advances in Pyroelectric Materials and Applications. *Small* **2021**, *17*, 2103960. [[CrossRef](#)]
5. Zhu, T.; Liu, Y.; Fu, C.; Heremans, J.P.; Snyder, J.G.; Zhao, X. Compromise and Synergy in High-Efficiency Thermoelectric Materials. *Adv. Mater.* **2017**, *29*, 1605884. [[CrossRef](#)]
6. Chen, Z.-G.; Shi, X.; Zhao, L.-D.; Zou, J. High-performance SnSe thermoelectric materials: Progress and future challenge. *Prog. Mater. Sci.* **2018**, *97*, 283–346. [[CrossRef](#)]
7. Zhao, L.-D.; Lo, S.-H.; Zhang, Y.; Sun, H.; Tan, G.; Uher, C.; Wolverton, C.; Dravid, V.P.; Kanatzidis, M.G. Ultralow thermal conductivity and high thermoelectric figure of merit in SnSe crystals. *Nature* **2014**, *508*, 373–377. [[CrossRef](#)]
8. Bell, L.E. Cooling, Heating, Generating Power, and Recovering Waste Heat with Thermoelectric Systems. *Science* **2008**, *321*, 1457–1461. [[CrossRef](#)]
9. Singh, G.; Sharma, M.; Sharma, J.D.; Kumar, S.; Vaish, R. Ferroelectric ceramics for pyrocatalytic applications. *Prog. Solid State Chem.* **2023**, *72*, 100428. [[CrossRef](#)]
10. de Vivanco, M.U.; Zschornak, M.; Stöcker, H.; Jachalke, S.; Mehner, E.; Leisegang, T.; Meyer, D.C. Pyroelectrically-driven chemical reactions described by a novel thermodynamic cycle. *Phys. Chem. Chem. Phys.* **2020**, *22*, 17781–17790. [[CrossRef](#)] [[PubMed](#)]
11. Liu, Y.; Wang, X.; Qiao, Y.; Min, M.; Wang, L.; Shan, H.; Ma, Y.; Hao, W.; Tao, P.; Shang, W.; et al. Pyroelectric Synthesis of Metal-BaTiO<sub>3</sub> Hybrid Nanoparticles with Enhanced Pyrocatalytic Performance. *ACS Sustain. Chem. Eng.* **2018**, *7*, 2602–2609. [[CrossRef](#)]

12. Schlechtweg, J.; Raufaisen, S.; Stelter, M.; Braeutigam, P. A novel model for pyro-electro-catalytic hydrogen production in pure water. *Phys. Chem. Chem. Phys.* **2019**, *21*, 23009–23016. [[CrossRef](#)]
13. Wu, Z.; Lou, W.; Zhang, H.; Jia, Y. Strong pyro-catalysis of shape-controllable bismuth oxychloride nanomaterial for wastewater remediation. *Appl. Sur. Sci.* **2020**, *513*, 145630. [[CrossRef](#)]
14. Xie, M.; Dunn, S.; Boulbar, E.L.; Bowen, C.R. Pyroelectric energy harvesting for water splitting. *Int. J. Hydrogen Energy* **2017**, *42*, 23437–23445. [[CrossRef](#)]
15. Zhang, H.; Zhang, S.; Yao, G.; Huang, Z.; Xie, Y.; Su, Y.; Yang, W.; Zheng, C.; Lin, Y. Simultaneously Harvesting Thermal and Mechanical Energies based on Flexible Hybrid Nanogenerator for Self-Powered Cathodic Protection. *ACS Appl. Mater. Interfaces* **2015**, *7*, 28142–28147. [[CrossRef](#)] [[PubMed](#)]
16. Zhang, Y.; Kumar, S.; Marken, F.; Krasny, M.; Roake, E.; Eslava, S.; Dunn, S.; Da Como, E.; Bowen, C.R. Pyro-electrolytic water splitting for hydrogen generation. *Nano Energy* **2019**, *58*, 183–191. [[CrossRef](#)]
17. Zhang, Y.; Xie, M.; Adamaki, V.; Khanbareh, H.; Bowen, C.R. Control of electro-chemical processes using energy harvesting materials and devices. *Chem. Soc. Rev.* **2017**, *46*, 7757–7786. [[CrossRef](#)] [[PubMed](#)]
18. Wang, Y.; Wang, S.; Meng, Y.; Liu, Z.; Li, D.; Bai, Y.; Yuan, G.; Wang, Y.; Zhang, X.; Li, X.; et al. Pyro-catalysis for tooth whitening via oral temperature fluctuation. *Nat. Commun.* **2022**, *13*, 4419. [[CrossRef](#)] [[PubMed](#)]
19. You, H.; Jia, Y.; Wu, Z.; Wang, F.; Huang, H.; Wang, Y. Room-temperature pyro-catalytic hydrogen generation of 2D few-layer black phosphorene under cold-hot alternation. *Nat. Commun.* **2018**, *9*, 2889. [[CrossRef](#)]
20. Achour, A.; Chen, K.; Reece, M.J.; Huang, Z. Tuning of Catalytic Activity by Thermoelectric Materials for Carbon Dioxide Hydrogenation. *Adv. Energy Mater.* **2018**, *8*, 1701430. [[CrossRef](#)]
21. Achour, A.; Liu, J.; Peng, P.; Shaw, C.; Huang, Z. In Situ Tuning of Catalytic Activity by Thermoelectric Effect for Ethylene Oxidation. *ACS Catal.* **2018**, *8*, 10164–10172. [[CrossRef](#)]
22. Lin, Y.-J.; Khan, I.; Saha, S.; Wu, C.-C.; Barman, S.R.; Kao, F.-C.; Lin, Z.-H. Thermocatalytic hydrogen peroxide generation and environmental disinfection by Bi<sub>2</sub>Te<sub>3</sub> nanoplates. *Nat. Commun.* **2021**, *12*, 180. [[CrossRef](#)] [[PubMed](#)]
23. Dong, Y.; Dong, S.; Yu, C.; Liu, J.; Gai, S.; Xie, Y.; Zhao, Z.; Qin, X.; Feng, L.; Yang, P.; et al. Mitochondria-targeting Cu<sub>3</sub>V<sub>5</sub>S<sub>4</sub> nanostructure with high copper ionic mobility for photothermoelectric therapy. *Sci. Adv.* **2023**, *9*, eadi9980. [[CrossRef](#)] [[PubMed](#)]
24. Sharifi, T.; Zhang, X.; Costin, G.; Yazdi, S.; Woellner, C.F.; Liu, Y.; Tiwary, C.S.; Ajayan, P. Thermoelectricity Enhanced Electrocatalysis. *Nano Lett.* **2017**, *17*, 7908–7913. [[CrossRef](#)] [[PubMed](#)]
25. Wang, S.; Qiao, Y.; Liu, X.; Zhu, S.; Zheng, Y.; Jiang, H.; Zhang, Y.; Shen, J.; Li, Z.; Liang, Y.; et al. Reduced Graphene Oxides Modified Bi<sub>2</sub>Te<sub>3</sub> Nanosheets for Rapid Photo-Thermoelectric Catalytic Therapy of Bacteria-Infected Wounds. *Adv. Funct. Mater.* **2023**, *33*, 2210098. [[CrossRef](#)]
26. Jiang, X.; Yang, M.; Fang, Y.; Yang, Z.; Dai, X.; Gu, P.; Feng, W.; Chen, Y. A Photo-Activated Thermoelectric Catalyst for Ferroptosis-/Pyroptosis-Boosted Tumor Nanotherapy. *Adv. Healthc. Mater.* **2023**, *12*, 2300699. [[CrossRef](#)] [[PubMed](#)]
27. Li, S.; Zhao, Z.; Zhao, J.; Zhang, Z.; Li, X.; Zhang, J. Recent Advances of Ferro-, Piezo-, and Pyroelectric Nanomaterials for Catalytic Applications. *ACS Appl. Nano Mater.* **2020**, *3*, 1063–1079. [[CrossRef](#)]
28. Zhang, Y.; Phuong, P.T.T.; Roake, E.; Khanbareh, H.; Wang, Y.; Dunn, S.; Bowen, C. Thermal Energy Harvesting Using Pyroelectric-Electrochemical Coupling in Ferroelectric Materials. *Joule* **2020**, *4*, 301–309. [[CrossRef](#)]
29. Wang, C.; Tian, N.; Ma, T.; Zhang, Y.; Huang, H. Pyroelectric catalysis. *Nano Energy* **2020**, *78*, 105371. [[CrossRef](#)]
30. Wang, J.; Hu, C.; Shi, L.; Tian, N.; Huang, H.; Ou, H.; Zhang, Y. Energy and environmental catalysis driven by stress and temperature-variation. *J. Mater. Chem. A* **2021**, *9*, 12400–12432. [[CrossRef](#)]
31. Achour, A. In-Situ Tuning of Catalytic Activity by Thermoelectric Effect. Ph.D. Thesis, Cranfield University, Bedford, UK, 2017.
32. Xu, X.; Xiao, L.; Jia, Y.; Wu, Z.; Wang, F.; Wang, Y.; Haugen, N.O.; Huang, H. Pyro-catalytic hydrogen evolution by Ba<sub>0.7</sub>Sr<sub>0.3</sub>TiO<sub>3</sub> nanoparticles: Harvesting cold-hot alternation energy near room-temperature. *Energy Environ. Sci.* **2018**, *11*, 2198–2207. [[CrossRef](#)]
33. Yang, Y.; Zhang, H.; Lee, S.; Kim, D.; Hwang, W.; Wang, Z.L. Hybrid Energy Cell for Degradation of Methyl Orange by Self-Powered Electrocatalytic Oxidation. *Nano Lett.* **2013**, *13*, 803–808. [[CrossRef](#)]
34. Wu, J.; Mao, W.; Wu, Z.; Xu, X.; You, H.; Xue, A.X.; Jia, Y. Strong pyro-catalysis of pyroelectric BiFeO<sub>3</sub> nanoparticles under a room-temperature cold-hot alternation. *Nanoscale* **2016**, *8*, 7343–7350. [[CrossRef](#)]
35. Kakekhani, A.; Ismail-Beigi, S. Polarization-driven catalysis via ferroelectric oxide surfaces. *Phys. Chem. Chem. Phys.* **2016**, *18*, 19676–19695. [[CrossRef](#)] [[PubMed](#)]
36. Kakekhani, A.; Ismail-Beigi, S. Ferroelectric oxide surface chemistry: Water splitting via pyroelectricity. *J. Mater. Chem. A* **2016**, *4*, 5235–5246. [[CrossRef](#)]
37. Kakekhani, A.; Ismail-Beigi, S.; Altman, E.I. Ferroelectrics: A pathway to switchable surface chemistry and catalysis. *Surf. Sci.* **2016**, *650*, 302–316. [[CrossRef](#)]
38. Min, M.; Liu, Y.; Song, C.; Zhao, D.; Wang, X.; Qiao, Y.; Feng, R.; Hao, W.; Tao, P.; Shang, W.; et al. Photothermally Enabled Pyro-Catalysis of a BaTiO<sub>3</sub> Nanoparticle Composite Membrane at the Liquid/Air Interface. *ACS Appl. Mater. Interfaces* **2018**, *10*, 21246–21253. [[CrossRef](#)]
39. Qian, W.; Wu, Z.; Jia, Y.; Hong, Y.; Xu, X.; You, H.; Zheng, Y.; Xia, Y. Thermo-electrochemical coupling for room temperature thermocatalysis in pyroelectric ZnO nanorods. *Electrochem. Commun.* **2017**, *81*, 124–127. [[CrossRef](#)]

40. Zhang, M.; Hu, Q.; Ma, K.; Ding, Y.; Li, C. Pyroelectric effect in CdS nanorods decorated with a molecular Co-catalyst for hydrogen evolution. *Nano Energy* **2020**, *73*, 104810. [[CrossRef](#)]
41. You, H.; Li, S.; Fan, Y.; Guo, X.; Lin, Z.; Ding, R.; Cheng, X.; Zhang, H.; Lo, T.W.B.; Hao, J.; et al. Accelerated pyro-catalytic hydrogen production enabled by plasmonic local heating of Au on pyroelectric BaTiO<sub>3</sub> nanoparticles. *Nat. Commun.* **2022**, *13*, 6144. [[CrossRef](#)]
42. Xiao, L.; Xu, X.; Jia, Y.; Hu, G.; Hu, J.; Yuan, B.; Yu, Y.; Zou, G. Pyroelectric nanoplates for reduction of CO<sub>2</sub> to methanol driven by temperature-variation. *Nat. Commun.* **2021**, *12*, 318. [[CrossRef](#)] [[PubMed](#)]
43. Dashevsky, Z.; Jarashneli, A.; Unigovski, Y.; Dzunzda, B.; Gao, F.; Shneck, R.Z. Development of a High Performance Gas Thermoelectric Generator (TEG) with Possible Use of Waste Heat. *Energies* **2022**, *15*, 3960. [[CrossRef](#)]
44. Sootsman, J.R.; Chung, D.Y.; Kanatzidis, M.G. New and old concepts in thermoelectric materials. *Angew. Chem. Int. Ed.* **2009**, *48*, 8616–8639. [[CrossRef](#)]
45. Zheng, Z.-H.; Shi, X.-L.; Ao, D.-W.; Liu, W.-D.; Li, M.; Kou, L.-Z.; Chen, Y.-X.; Li, F.; Wei, M.; Liang, G.-X.; et al. Harvesting waste heat with flexible Bi<sub>2</sub>Te<sub>3</sub> thermoelectric thin film. *Nat. Sustain.* **2023**, *6*, 180–191. [[CrossRef](#)]
46. Dashevsky, Z.; Skipidarov, S. Investigating the Performance of Bismuth-Antimony Telluride. In *Novel Thermoelectric Materials and Device Design Concepts*; Skipidarov, S., Nikitin, M., Eds.; Springer International Publishing: Cham, Switzerland, 2019; pp. 3–21.
47. Tritt, T.M.; Subramanian, M.A. Thermoelectric Materials, Phenomena, and Applications: A Bird's Eye View. *MRS Bull.* **2011**, *31*, 188–198. [[CrossRef](#)]
48. Snyder, G.J.; Toberer, E.S. Complex thermoelectric materials. In *Materials for Sustainable Energy*; Nature Publishing Group: New York, NY, USA, 2010; pp. 101–110.
49. Zhao, L.D.; Zhang, B.P.; Li, J.F.; Zhang, H.L.; Liu, W.S. Enhanced thermoelectric and mechanical properties in textured n-type Bi<sub>2</sub>Te<sub>3</sub> prepared by spark plasma sintering. *Solid State Sci.* **2008**, *10*, 651–658. [[CrossRef](#)]
50. Zhao, L.-D.; Zhang, B.-P.; Li, J.-F.; Zhou, M.; Liu, W.-S.; Liu, J. Thermoelectric and mechanical properties of nano-SiC-dispersed Bi<sub>2</sub>Te<sub>3</sub> fabricated by mechanical alloying and spark plasma sintering. *J. Alloys Compd.* **2008**, *455*, 259–264. [[CrossRef](#)]
51. Cao, T.; Shi, X.-L.; Li, M.; Hu, B.; Chen, W.; Liu, W.-D.; Lyu, W.; MacLeod, J.; Chen, Z.-G. Advances in bismuth-telluride-based thermoelectric devices: Progress and challenges. *eScience* **2023**, *3*, 100122. [[CrossRef](#)]
52. Pei, Y.; Shi, X.; LaLonde, A.; Wang, H.; Chen, L.; Snyder, G.J. Convergence of electronic bands for high performance bulk thermoelectrics. *Nature* **2011**, *473*, 66–69. [[CrossRef](#)]
53. Zhao, L.D.; Wu, H.J.; Hao, S.Q.; Wu, C.I.; Zhou, X.Y.; Biswas, K.; He, J.Q.; Hogan, T.P.; Uher, C.; Wolverton, C.; et al. All-scale hierarchical thermoelectrics: MgTe in PbTe facilitates valence band convergence and suppresses bipolar thermal transport for high performance. *Energy Environ. Sci.* **2013**, *6*, 3346–3355. [[CrossRef](#)]
54. Chang, C.; Wang, D.; He, D.; He, W.; Zhu, F.; Wang, G.; He, J.; Zhao, L.D. Realizing High-Ranged Out-of-Plane ZTs in N-Type SnSe Crystals through Promoting Continuous Phase Transition. *Adv. Energy Mater.* **2019**, *9*, 1901334. [[CrossRef](#)]
55. Qin, B.; Wang, D.; He, W.; Zhang, Y.; Wu, H.; Pennycook, S.J.; Zhao, L.-D. Realizing High Thermoelectric Performance in p-Type SnSe through Crystal Structure Modification. *J. Am. Chem. Soc.* **2018**, *141*, 1141–1149. [[CrossRef](#)]
56. Zhang, X.; Feng, D.; He, J.; Zhao, L.-D. Attempting to realize n-type BiCuSeO. *J. Solid State Chem.* **2018**, *258*, 510–516. [[CrossRef](#)]
57. Zhao, L.D.; Berardan, D.; Pei, Y.L.; Byl, C.; Pinsard-Gaudart, L.; Drago, N. Bi<sub>1-x</sub>Sr<sub>x</sub>CuSeO oxyselenides as promising thermoelectric materials. *Appl. Phys. Lett.* **2010**, *97*, 092118. [[CrossRef](#)]
58. Liu, Y.; Li, M.; Wan, S.; Lim, K.H.; Zhang, Y.; Li, M.; Li, J.; Ibáñez, M.; Hong, M.; Cabot, A. Surface Chemistry and Band Engineering in AgSbSe<sub>2</sub>: Toward High Thermoelectric Performance. *ACS Nano* **2023**, *17*, 11923–11934. [[CrossRef](#)]
59. Burmistrov, I.; Khanna, R.; Gorshkov, N.; Kiselev, N.; Artyukhov, D.; Boychenko, E.; Yudin, A.; Konyukhov, Y.; Kravchenko, M.; Gorokhovskiy, A.; et al. Advances in Thermo-Electrochemical (TEC) Cell Performances for Harvesting Low-Grade Heat Energy: A Review. *Sustainability* **2022**, *14*, 9483. [[CrossRef](#)]
60. Ohta, T.; Asakura, S.; Yamaguchi, M.; Kamiya, N.; Gotgh, N.; Otagawa, T. Photochemical and thermoelectric utilization of solar energy in a hybrid water-splitting system. *Int. J. Hydrogen Energy* **1976**, *1*, 113–116. [[CrossRef](#)]
61. Ohta, T.; Kamiya, N.; Yamaguchi, M.; Gotoh, N.; Otagawa, T.; Asakura, S. System efficiency of a water-splitting system synthesized by photochemical and thermoelectric conversion of solar energy. *Int. J. Hydrogen Energy* **1978**, *3*, 203–208. [[CrossRef](#)]
62. Pornrunroj, C.; Andrei, V.; Reiser, E. Thermoelectric-Photoelectrochemical Water Splitting under Concentrated Solar Irradiation. *J. Am. Chem. Soc.* **2023**, *145*, 13709–13714. [[CrossRef](#)]
63. Shi, X.-L.; Zou, J.; Chen, Z.-G. Advanced Thermoelectric Design: From Materials and Structures to Devices. *Chem. Rev.* **2020**, *120*, 7399–7515. [[CrossRef](#)]
64. He, P.; Zhang, L.; Wu, L.; Xiao, S.; Ren, X.; He, R.; Yang, X.; Liu, R.; Duan, T. Synergy of oxygen vacancies and thermoelectric effect enhances uranium(VI) photoreduction. *Appl. Catal. B Environ.* **2023**, *322*, 122087. [[CrossRef](#)]
65. Zheng, X.; Cao, Y.; Wang, H.; Zhang, J.; Zhao, M.; Huang, Z.; Wang, Y.; Zhang, L.; Deng, Y.; Hu, W.; et al. Designing Breathing Air-electrode and Enhancing the Oxygen Electrocatalysis by Thermoelectric Effect for Efficient Zn-air Batteries. *Angew. Chem. Int. Ed.* **2023**, *62*, e202302689. [[CrossRef](#)]
66. Ji, X.; Tang, Z.; Liu, H.; Kang, Y.; Chen, L.; Dong, J.; Chen, W.; Kong, N.; Tao, W.; Xie, T. Nanoheterojunction-Mediated Thermoelectric Strategy for Cancer Surgical Adjuvant Treatment and β-Element Combination Therapy. *Adv. Mater.* **2023**, *35*, 2207391. [[CrossRef](#)]

67. Pan, C.; Ou, M.; Wang, Y.; Xiao, Q.; Mei, L.; Ji, X. p-n Heterojunction-based Thermoelectric Generator for Highly Efficient Cancer Thermoelectric Therapy. *Res. Sq.* **2021**, preprint. [[CrossRef](#)]
68. Yuan, X.; Kang, Y.; Dong, J.; Li, R.; Ye, J.; Fan, Y.; Han, J.; Yu, J.; Ni, G.; Ji, X.; et al. Self-triggered thermoelectric nanoheterojunction for cancer catalytic and immunotherapy. *Nat. Commun.* **2023**, *14*, 5140. [[CrossRef](#)] [[PubMed](#)]
69. Li, S.; Zhao, Z.; Li, J.; Liu, H.; Liu, M.; Zhang, Y.; Su, L.; Pérez-Jiménez, A.I.; Guo, Y.; Yang, F.; et al. Mechanically Induced Highly Efficient Hydrogen Evolution from Water over Piezoelectric SnSe nanosheets. *Small* **2022**, *18*, 2202507. [[CrossRef](#)] [[PubMed](#)]
70. Li, S.; Zhao, Z.; Liu, M.; Liu, X.; Huang, W.; Sun, S.; Jiang, Y.; Liu, Y.; Zhang, J.; Zhang, Z. Remarkably enhanced photocatalytic performance of Au/AgNbO<sub>3</sub> heterostructures by coupling piezotronic with plasmonic effects. *Nano Energy* **2022**, *95*, 107031. [[CrossRef](#)]
71. Zhang, Y.; Ohta, H. Electron Sandwich Doubles the Thermoelectric Power Factor of SrTiO<sub>3</sub>. *Phys. Status Solidi A* **2019**, *216*, 1800832. [[CrossRef](#)]
72. Zhang, Y.; Sugo, K.; Cho, H.J.; Ohta, H. Thermoelectric phase diagram of the SrTiO<sub>3</sub>-LaTiO<sub>3</sub> solid-solution system through a metal to Mott insulator transition. *J. Appl. Phys.* **2019**, *126*, 07510. [[CrossRef](#)]
73. Zhang, Y.; Feng, B.; Hayashi, H.; Tohei, T.; Tanaka, I.; Ikuhara, Y.; Ohta, H. Thermoelectric phase diagram of the SrTiO<sub>3</sub>-SrNbO<sub>3</sub> solid solution system. *J. Appl. Phys.* **2017**, *121*, 185102. [[CrossRef](#)]
74. Hicks, L.D.; Dresselhaus, M.S. Effect of quantum-well structures on the thermoelectric figure of merit. *Phys. Rev. B* **1993**, *47*, 12727–12731. [[CrossRef](#)] [[PubMed](#)]
75. Hicks, L.D.; Dresselhaus, M.S. Thermoelectric figure of merit of a one-dimensional conductor. *Phys. Rev. B* **1993**, *47*, 16631–16634. [[CrossRef](#)] [[PubMed](#)]
76. Zhang, Y.Q.; Feng, B.; Hayashi, H.; Chang, C.P.; Sheu, Y.M.; Tanaka, I.; Ikuhara, Y.; Ohta, H. Double thermoelectric power factor of a 2D electron system. *Nat. Commun.* **2018**, *9*, 2224. [[CrossRef](#)] [[PubMed](#)]

**Disclaimer/Publisher's Note:** The statements, opinions and data contained in all publications are solely those of the individual author(s) and contributor(s) and not of MDPI and/or the editor(s). MDPI and/or the editor(s) disclaim responsibility for any injury to people or property resulting from any ideas, methods, instructions or products referred to in the content.